

# Climbing Jacob's Ladder in the Warm Dense Environment: Generalized Gradient Approximation Exchange-Correlation Free-Energy Functional

Valentin V. Karasiev,<sup>1,\*</sup> James W. Dufty,<sup>2</sup> and S.B. Trickey<sup>1</sup>

<sup>1</sup>*Quantum Theory Project, Department of Physics and Department of Chemistry,  
P.O. Box 118435, University of Florida, Gainesville FL 32611-8435*

<sup>2</sup>*Department of Physics, P.O. Box 118435, University of Florida, Gainesville FL 32611-8435  
(Dated: 19 Dec. 2016)*

The potential for density functional theory (DFT) calculations to address, reliably, the extreme conditions of warm dense matter (WDM) is predicated upon having an accurate representation for the exchange-correlation (XC) free energy functional. To that end, we give a systematic, constraint-based construction of a non-empirical finite-temperature (T) generalized gradient approximation (GGA), based on the XC free energy gradient expansion. The new functional provides the correct T-dependence in the slowly varying regime and the correct zero-T, high-T, and homogeneous electron gas limits. Kohn-Sham calculations with finite-T XC functionals (the new GGA and the local density approximation (LDA)), with ground state (LDA and GGA) functionals, and with a previously published mixed ground state GGA and finite-T LDA functional on a static fcc Aluminum lattice with hot electrons demonstrate the combined magnitude of thermal and gradient effects accounted for by the finite-T GGA functional. Accuracy of the new GGA functional in the WDM regime is illustrated by deuterium equation of state calculations in excellent agreement with reference path integral Monte Carlo results at intermediate and elevated T.

*Introduction.* The region of condensed system state conditions between ordinary condensed matter and plasmas, the so-called warm dense matter (WDM) regime, is characterized by elevated temperature and a wide range of pressures. Usually WDM is treated by means of finite-temperature density functional theory (DFT) [1–6] in the larger setting of ab initio molecular dynamics (AIMD, also called Born-Oppenheimer MD) [7–10].

Reliable approximations for the exchange-correlation (XC) free-energy density functional are required in practice. For the ground state there are literally hundreds of approximate XC functionals developed for molecular and condensed matter applications. In contrast, there are only a few approximate XC free-energy functionals. These include the random-phase approximation and classical mapping functionals [11, 12] and a scheme [13] which treats the gradient dependence by a ground-state generalized gradient approximation (GGA)  $E_{xc}^{GGA}$  with explicit T-dependence only from the local-density approximation (LDA) XC free energy:  $\mathcal{F}_{xc}^{GGA}[n, T] \approx \mathcal{F}_{xc}^{LDA}[n, T] + E_{xc}^{GGA}[n] - E_{xc}^{LDA}[n]$ . Discussion of that mixture, which we denote as SD14, is below. The LDA used for the XC free-energy [14] is our recently developed, accurate parametrization (“KSDT”) of path-integral Monte Carlo (PIMC) data for the homogeneous electron gas (HEG) at finite-T [15]. Calculations using KSDT show that thermal XC effects are important for the direct current conductivity and the equation of state under certain thermodynamic conditions [17, 18]. Ref. 18 also showed that accurate predictions require an XC free-energy functional which incorporates both intrinsic T and inhomogeneity effects, hence a need for a finite-T GGA XC functional, the rung above LDA on the Perdew-Schmidt Jacob’s ladder functional hierarchy [19]. Earlier work [17, 20] on

thermal Hartree-Fock is consistent with that finding.

Development of non-empirical functionals beyond the LDA involves identification of appropriate T-dependent variables and constraints to enforce exact properties. Ref. 21 gave such a framework for construction of a GGA for the non-interacting free-energy, including generalization of T = 0K parametrization variables to T > 0K. That framework was used in building the VT84F non-interacting free-energy GGA [22]. Subsequent work on the LDA XC free-energy functional [14] made clear that constructing a proper, constraint-based GGA XC free-energy functional should parallel that path, adapted appropriately for the XC free energy exact properties.

Systematic construction of a GGA XC free energy rests on three requisites: (a) The finite-T LDA XC [14] makes the dominant contribution. Thus in the HEG and high-T limits the GGA XC must reduce to finite-T LDA, which is to say that high-T effects incorporated in the LDA XC free energy prevail over the inhomogeneity effects (gradient contributions) there. (b) The gradient expansion (GE) for the XC free-energy defines T-dependent variables (as analogues of the T=0 K reduced density gradient variables) to be used in the GGA enhancement factors for X and C such that the GGA functional reproduces the GE T-dependence in the weakly inhomogeneous electron gas regime. (c) As T → 0 K, the XC free-energy reduces to a ground-state functional which satisfies known constraints for the ground-state XC energy.

Regarding item (c), although there are substantially more refined non-empirical ground-state GGA XC functionals [23], here we choose to recover the extremely widely used PBE functional [24]. This selection facilitates use of existing computational resources such as PAW data sets and pseudopotentials. The XC free-

energy functional then is constructed by adding finite-T constraints to those for the ground-state used to determine the PBE form. Those additional constraints correspond to items (a) and (b) just described.

*Finite-T gradient expansion.* The second-order gradient correction for the XC free-energy density may be written similarly to the ground-state form [25, 26] as

$$nf_{xc}^{(2)}(n, \nabla n, T) = \frac{1}{2}g_{xc}^{(2)}(n, T)|\nabla n(\mathbf{r})|^2. \quad (1)$$

For ground-state GGA functionals the appropriate reduced density gradient variable is  $s = |\nabla n|/2(3\pi^2)^{1/3}n^{4/3}$ , so we re-express (1) in terms of  $s$  and make the conventional separation into X and C contributions,

$$f_{xc}^{(2)}(n, \nabla n, T) = C_x^{(2)}\varepsilon_x^{\text{LDA}}(n)s^2(n, \nabla n)\tilde{B}_x(t) + C_c^{(2)}n^{1/3}s^2(n, \nabla n)\tilde{B}_c(n, t). \quad (2)$$

It is important to note that the gradient correction for X factors into a product of the familiar  $s^2$  and a function of reduced temperature  $t = T/T_F \equiv 2k_B T/[3\pi^2 n]^{2/3} = (2/3)^{2/3}I_{1/2}^{-2/3}(\beta\mu)$ , with  $T_F$  the Fermi temperature. Here  $\beta \equiv 1/k_B T$  is the dimensionless inverse temperature,  $I_k$  is a Fermi-Dirac integral [27, 28],  $\varepsilon_x^{\text{LDA}}$  is the ground-state LDA exchange energy per electron, and  $B_x(t)$  is a combination of Fermi-Dirac integrals (details below), hence a function of  $t$  alone. The C term has a form similar to the X term, but with  $\tilde{B}_c$  dependent upon both  $n$  and  $t$ . Coefficient values of  $C_x^{(2)} = 8/81$  and  $C_c^{(2)} = 0.162125$  correspond, respectively, to the X free-energy [29] (see Eqs. (5)-(6) discussed below) and the  $T=0K$  C energy for the non-polarized slowly-varying electron gas [30]. Because of the special role that exchange plays in the Kohn-Sham decomposition, we start with development of the finite-T GGA for X.

*Finite-T GGA exchange.* GGA functionals are defined with respect to LDA. The LDA for the X free-energy per particle, obtained from the HEG with chemical potential  $\mu$  at inverse temperature  $\beta$ , has the factorized form [31]

$$f_x^{\text{LDA}}(n, T) = \varepsilon_x^{\text{LDA}}(n)\tilde{A}_x(t), \quad (3)$$

where

$$\tilde{A}_x(t) = \frac{t^2}{2} \int_{-\infty}^{(\beta\mu)} I_{-1/2}^2(\eta) d\eta, \quad (4)$$

is an implicit function of  $t$ .

To exploit this factorized property of the LDA, the second-order gradient expansion (GE2) for the X free energy (corresponding to Eq. (2)) can be written [29, 32–35] as

$$f_x^{\text{GE2}}(n, \nabla n, T) = f_x^{\text{LDA}}(n, T) \left( 1 + \frac{8}{81} \frac{\tilde{B}_x(t)}{\tilde{A}_x(t)} s^2(n, \nabla n) \right). \quad (5)$$

(Remark: whether the coefficient is 8/81 or 10/81 as from the ground-state analysis [36] is irrelevant here, since we must match the small- $s^2$  behavior of the ground-state GGA X functional chosen for the  $T \rightarrow 0K$  limit. Here that is PBE.) The explicit form of  $\tilde{B}_x(t)$  is

$$\tilde{B}_x(t) = \left(\frac{3}{2}\right)^{4/3} I_{1/2}^{4/3}(\beta\mu) \left[ \left( \frac{I'_{-1/2}(\beta\mu)}{I_{-1/2}(\beta\mu)} \right)^2 - 3 \frac{I''_{-1/2}(\beta\mu)}{I_{-1/2}(\beta\mu)} \right]. \quad (6)$$

Primes indicate differentiation with respect to the argument. Details as well as accurate fits for  $\tilde{A}_x$  and  $\tilde{B}_x$  as explicit functions of  $y \equiv 2/3t^{3/2}$  (or functions of  $t$  after a change of variable) are given in Ref. 37.

The strategy for building a GGA is to generalize the GE2 (and avoid its deficiencies) by identifying an appropriate reduced gradient variable from within the GE2, then defining the approximation as the LDA (zeroth-order term) multiplied by a dimensionless enhancement factor which is a function of that reduced gradient variable. In the finite-T case, the GE2 for X, Eq. (5), identifies the corresponding finite-T reduced density gradient for the X free-energy as

$$s_{2x}(n, \nabla n, T) \equiv s^2(n, \nabla n) \frac{\tilde{B}_x(t)}{\tilde{A}_x(t)}. \quad (7)$$

(Remark: we cannot define the appropriate variable in terms of  $s$  because  $\tilde{B}_x(t)$  has both signs; see below.) Then the finite-T X free-energy GGA becomes

$$\mathcal{F}_x^{\text{GGA}}[n, T] = \int n f_x^{\text{LDA}}(n, T) F_x(s_{2x}) d\mathbf{r}. \quad (8)$$

Evidently Eq. (8) is a generalization of the GE2 X free-energy, Eq. (5). It is straightforward to show that in the zero-temperature limit

$$\lim_{T \rightarrow 0} s_{2x}(n, \nabla n, T) = s^2(n, \nabla n). \quad (9)$$

The left-hand panel of Figure 1 shows both  $\tilde{A}_x$  and the ratio  $s_{2x}/s^2 \equiv \tilde{B}_x/\tilde{A}_x$  as functions of  $t$ .  $\tilde{A}_x$  vanishes in the high-T limit, but  $\tilde{B}_x$  decays more rapidly (see Ref. [37] for the relevant asymptotic expansions) such that the ratio  $\tilde{B}_x/\tilde{A}_x$  eventually vanishes as well. That guarantees satisfaction of the correct high-T limit for X (provided that  $F_x(0) = 1$ ; see additional comments below Eq. (10)). Further, the definition Eq. (8) guarantees that the X free-energy scales correctly [38, 39],  $\mathcal{F}_x^{\text{GGA}}[n_\lambda, T] = \lambda \mathcal{F}_x^{\text{GGA}}[n, T/\lambda^2]$ , with  $n_\lambda(\mathbf{r}) = \lambda^3 n(\lambda\mathbf{r})$ .

Because of the limit given by Eq. (9), the simplest approximation for a finite-T X enhancement factor  $F_x(s_{2x})$  might seem to be use of a zero-T GGA X enhancement factor. That would guarantee achievement of item (c) above. However, the distinctive sign change of  $s_{2x}$  near  $t = 1$ , Fig. 1, precludes straightforward adoption of popular choices such as the PBE enhancement factor [24] because of the unphysical poles that could result. A more refined generalization to finite-T is required.

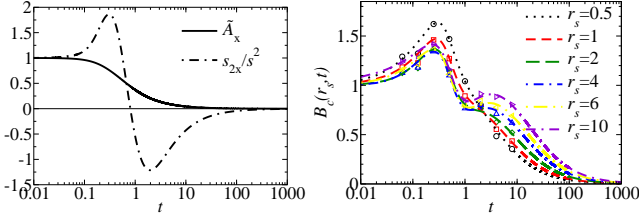


FIG. 1: Left: Behavior of  $\tilde{A}_x$  and  $s_{2x}/s^2 \equiv \tilde{B}_x/\tilde{A}_x$  as functions of  $t$ . Right: Behavior of  $\tilde{B}_c(r_s, t)$  shown as comparison between the reference data (symbols) and Padé fit (Eq. (11); curves) for selected  $r_s$  values.

We construct a well-behaved X enhancement factor by imposition of the following detailed constraints: [i]  $F_x(0) = 1$  to recover the HEG limit both at zero- and at finite-T; [ii] recovery of the T-dependence of the GE2 in the small- $s$  limit  $F_x(s_{2x}) \approx 1 + \nu_x s_{2x}$  with  $\nu_x$  a constant consistent with the  $s^2$  coefficient in the T=0K limit GGA (here PBE); [iii] local satisfaction of the zero-T Lieb-Oxford bound [40] by requiring  $F_x(s_{2x}) \leq F_{x,\max} = 1.804$  (see [24]); [iv] smooth, non-negative behavior for all  $s_{2x} \in ]-\infty, +\infty[$ , to match the behavior of exact exchange at finite-T [41].

A simple enhancement factor

$$F_x(s_{2x}) = 1 + \frac{\nu_x s_{2x}}{1 + \alpha |s_{2x}|}, \quad (10)$$

with  $\alpha = \nu_x/(F_{x,\max} - 1)$  satisfies all of those constraints. Additionally, (10) with suitably chosen constants recovers PBE X in the zero-T limit:  $s_{2x} \rightarrow s^2 \Rightarrow \lim_{T \rightarrow 0} F_x(s_{2x}) = 1 + \nu_x s^2/(1 + \alpha s^2)$ . In the high-T limit, the density-gradient dependence of  $s_{2x}$  is suppressed by the decaying tail of the  $\tilde{B}_x(t)/\tilde{A}_x(t)$  function (see Fig. 1), such that  $\lim_{T \rightarrow \infty} F_x(s_{2x}) = 1$ . Constraint [i] thus is satisfied not only for the strictly homogeneous case ( $s = 0$ ), but also for non-uniform densities with any finite  $s$  value. This property is correctly inherited by the finite-T GGA Eq. (10) from the GE2 Eq. (5).

*Finite-T GGA correlation.* As shown in Eq. (2), the C term is similar to X with the important difference that  $\tilde{B}_c$  depends upon both  $n$  and  $t$ .

The gradient correction  $g_{xc}^{(2)}(n, T)$  was evaluated numerically in Ref. [13] with use of a relation to the static local field correction [42, 43] and quantum Monte-Carlo data for the finite-T HEG [44]. Those data together with Eq. (2) allow us to evaluate  $\tilde{B}_c(r_s, t)$  ( $r_s = (3/4\pi)^{1/3} n^{-1/3}$ ) numerically. The result is consistent with the assumption that the correlation gradient correction in Eq. (2) reduces to the zero-T gradient correction when  $T \rightarrow 0$ , i.e., that  $\lim_{T \rightarrow 0} \tilde{B}_c(r_s, t) = 1$ . An analytical form for  $\tilde{B}_c(r_s, t)$  then can be obtained by a technique used earlier[37] that fits a Padé approximant of order [4, 5] with respect to the variable  $t$  and  $r_s$ -dependent

coefficients, to wit

$$\tilde{B}_c(r_s, t) = \frac{1 + \sum_{i=1}^4 (a_i + b_i r_s^{3/4} + c_i r_s^{3/2}) t^i}{1 + \sum_{i=1}^5 (d_i + e_i r_s + f_i r_s^2) t^i}. \quad (11)$$

This form incorporates the correct zero-T limit and decreases for large T. During parametrization,  $\tilde{B}_c(r_s, t)$  was checked for poles in the domain  $(r_s, t) \in ([0.01, 1000], [0, 1000])$ . If the denominator of Eq. (11) had a root, that parameter set was rejected. Proper positivity also was enforced. In addition to the reference data points shown in the right-hand panel of Fig. 1, we also used  $r_s = 12$  data with the same set of  $t$  values.

The right-hand panel of Figure 1 shows the outcome. Analytical results from Eq. (11) agree well with the reference data. The mean absolute relative error of the fit calculated over 64 reference points is 2%, while the maximum relative error is 13% at  $(r_s, t) = (0.5, 4)$ . The function  $\tilde{B}_c$  has smooth T and  $r_s$  dependencies, is everywhere positive, goes to unity in the zero- $t$  limit (by construction), and vanishes in the high-T limit (thereby guaranteeing satisfaction of the correct high-T limit for correlation).

With  $\tilde{B}_c$  in hand, the fact that the C term in Eq. (2) is proportional to  $n^{1/3} s^2 \tilde{B}_c(r_s, t) \propto q^2 \tilde{B}_c(r_s, t)$  (with  $q(n, \nabla n) = |\nabla n|/2k_s n$  the ground-state reduced density gradient for C and  $k_s = 2(3n/\pi)^{1/6}$  the Thomas-Fermi screening wave number; the seemingly peculiar dimensions are a result of Hartree a.u.) motivates definition of the T-dependent reduced density gradient for C as

$$q_c(n, \nabla n, T) = q(n, \nabla n) \sqrt{\tilde{B}_c(r_s, t)}, \quad (12)$$

In terms of  $q_c$ , the finite-T GGA correlation functional is formed by imposition of the following conditions. The functional must [v] provide the correct HEG limit both at zero- and at finite-T, hence must reduce to the LDA C (free-) energy; [vi] reproduce the slowly varying regime correctly; for  $T > 0$  the correct T-dependence in that regime is given by  $\tilde{B}_c$ ; [vii] satisfy known T=0K constraints for C (see Ref. [24] for example); [viii] reduce to the LDA C free energy in the high-T limit for any  $n$  with finite reduced gradient  $q$  (in consequence of the finite-T gradient expansion).

The simplest approximation which satisfies all these constraints is based on a known zero-T GGA correlation functional (which satisfies [vii]) with T-dependence introduced as follows. Adapt the PBE form of C energy per particle (spin-unpolarized case) to become

$$f_c^{\text{GGA}}(n, \nabla n, T) = f_c^{\text{LDA}}(n, T) + H\left(f_c^{\text{LDA}}, \zeta = 0, q_c\right), \quad (13)$$

where  $f_c^{\text{LDA}}$  is the LDA correlation free-energy per particle,  $\zeta$  is the spin polarization fraction, and  $H$  is as defined in PBE [24], but with substitutions as shown. Details are

TABLE I: Parameters for the  $\tilde{B}_c(r_s, t)$  fit, Eq. (11).

$i$	$a_i$	$b_i$	$c_i$
1	0.85305204E+01	0.24067020E+01	0.41084149E+01
2	-0.33204984E+02	0.59669251E+02	0.18565109E+01
3	0.77723154E+02	-0.11369432E+03	-0.66717859E+01
4	0.38024010E+02	0.77853520E+02	0.19171739E+02
	$d_i$	$e_i$	$f_i$
1	0.13031416E+00	0.11215998E+02	0.23161518E+00
2	0.42386943E-03	0.11310648E-01	0.24725876E-02
3	0.12554090E-01	0.11490731E-01	0.30851598E-02
4	0.46773371E+02	0.66434442E+02	0.67612929E+00
5	0.20633935E+02	0.37417733E+01	0.15211873E-06

in the Supplemental Material [45]. Thus the GGA correlation free-energy is  $\mathcal{F}_c^{\text{GGA}}[n, T] = \int n f_c^{\text{GGA}}(n, \nabla n, T) d\mathbf{r}$ . In the rapidly varying case the function  $f_c^{\text{GGA}}$  is vanishing due to properties of the ground state PBE C functional,  $\lim_{q_c \rightarrow \infty} H = -f_c^{\text{LDA}}$ . In the slowly varying regime, the function given in Eq. (13) recovers the second-order gradient expansion (see Refs. [24, 30]) with T-dependence described by  $\tilde{B}_c$ . In conjunction with the GE2 for X, that also provides the correct XC T-dependence defined by Eqs. (1)-(2).

The vanishing of  $\tilde{B}_c$  in the high-T limit provides satisfaction of requirement [viii] (analogously with the X case) for all densities with finite values of the variable  $q$ . This follows from  $\lim_{T \rightarrow \infty} H(f_c^{\text{LDA}}, \zeta, q_c) = 0$ . Thus the GGA XC free-energy functional,  $\mathcal{F}_{xc}^{\text{GGA}}[n, T] \equiv \mathcal{F}_x^{\text{GGA}}[n, T] + \mathcal{F}_c^{\text{GGA}}[n, T]$ , reduces in the high-T limit to the LDA XC free-energy (in the present case, the KSDT parametrization, but the result is general) and eventually vanishes,

$$\lim_{T \rightarrow \infty} (\mathcal{F}_{xc}^{\text{GGA}}[n, T] - \mathcal{F}_{xc}^{\text{LDA}}[n, T]) = 0, \quad (14)$$

for any density  $n$  with finite reduced gradients  $s$  and  $q$ . Remark: The SD14 mixed LDA-GGA functional exhibits this behavior only for uniform density.

We used PBE values,  $\nu_x = 0.21951$  in Eq. (10), and  $\beta_c = 0.066725$  in  $H$ , Eq. (13). (Remark: to avoid notational ambiguity,  $\nu_x$  and  $\beta_c$  here are the constants denoted  $\mu$  and  $\beta$  in Ref. [24].) Thus Eq. (8) reduces by construction to the ground-state PBE in the  $T=0$  K limit (except for the small differences between the PW-92 LDA [46] and the  $T=0$  K limit of KSDT).

*Results.* Figure 2 compares electronic pressure differences from three thermal XC functionals (present work denoted KDT16, SD14, and KSDT LDA) XC functionals and two ground-state functionals used with finite-T densities (PZ [47] LDA and PBE GGA). PZ is used as the comparison. The system is fcc Al over a wide range of  $T$ ,  $0 \leq T \leq 300$  kK at somewhat compressed material density  $\rho = 3$  g/cm<sup>3</sup>. Calculations were done with a locally modified version of Quantum Espresso [48]. Cal-

culations with the PZ and KSDT functionals used a projector augmented wave (PAW) data set built with PZ XC, while calculations with the PBE and T-dependent GGA (KDT16) employed the PBE PAW data set. All the calculations were otherwise self-consistent.

The pressure differences shown in Fig. 2 illuminate XC inhomogeneity effects in the case of  $P^{\text{PBE}} - P^{\text{PZ}}$ , thermal XC effects at the LDA level of refinement for  $P^{\text{KSDT}} - P^{\text{PZ}}$ , and the combined XC effects at the GGA level of refinement in  $(P^{\text{KDT16}} - P^{\text{PZ}})$ . The new KDT16 functional interpolates smoothly between the PBE values at low-T and the KSDT values at high-T (not fully shown). Pressure differences from both KDT16 (GGA) and from KSDT (LDA) have their maximum magnitude at intermediate-T, then decrease. We note that the ground state approximation, i.e.  $\mathcal{F}_{xc}^{\text{GGA}} \approx E_{xc}^{\text{PBE}}[n(T)]$  systematically overestimates the pressure by as much as  $\approx 10\%$  at  $T$  between  $\approx 40$  and 100 kK. Eventually the pressures from all proper functionals should go to a common high-T limit as the XC contribution becomes negligible compared to the non-interacting free-energy.

Fig. 2 also shows that pressures from the SD14 functional [13] have weaker T-dependence (relative to PZ XC) than do pressures from KSDT, whereas the new KDT16 full GGA gives about 30% bigger maximum pressure swing (also relative to PZ XC) than does KSDT. Note also that SD14 pressures start to deviate significantly from the values given by KDT16 at  $T = 50$  kK ( $t \approx 0.27$ ), a relative temperature that may be construed at least roughly as the beginning of the WDM regime.

As a further probe of accuracy of the new thermal GGA XC in a problem also of WDM relevance, we performed AIMD simulations for deuterium at two material densities over a wide  $T$  range. The PBE PAW data set was used and only the  $\Gamma$  point was sampled. Figure 3 compares results from the new KDT16 XC with those from PBE in the ground-state approximation, and reference PIMC simulations [49]. PBE again systematically over-estimates the pressure. The deviation becomes significant at  $T \approx 30$  kK for both material densities. The KDT16 XC provides excellent agreement with the reference PIMC values for  $T \geq 60$  kK. Discrepancies at  $T = 15$  and 30 kK are, we suspect, attributable to PIMC difficulties at low  $T$  (see Ref. [18]). Although the material density is quite different, note that SD14 [13] gave *higher* pressures than ground-state-approximation PBE up to  $T \approx 50$  kK in compressed deuterium. This is the reverse of the SD14 behavior for Al shown in Fig. 2. The difference may be rooted in the underlying distinction in T-dependence. The SD14 functional can produce only the implicit dependence of  $s[n(T)]$  but not the T-dependence of  $\tilde{B}_x$  or  $\tilde{B}_c$ . In SD14 deuterium calculations [13] the reduced temperature range was about  $0.02 \leq t \leq 0.2$ . As shown in Fig. 1, both  $\tilde{B}_x$  and  $\tilde{B}_c$  have positive  $t$  derivatives and non-trivial deviation from unity in that range.

*Summary.* We have constructed a non-empirical GGA



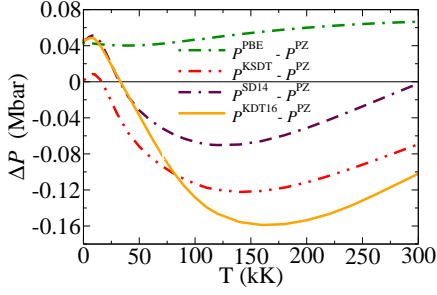


FIG. 2: Electronic pressure differences as a function of  $T$  for the new KDT16 GGA, SD14 mixed LDA-GGA, KSDT LDA, and ground-state PBE XC functionals, all referenced to PZ ground-state LDA values (self-consistent  $n(T)$  for each functional). Static lattice fcc Aluminum at  $3.0 \text{ g/cm}^3$ . SD14 results begin to deviate from KDT16 values for  $T=50 \text{ kK} \approx 0.27 T_F$ .

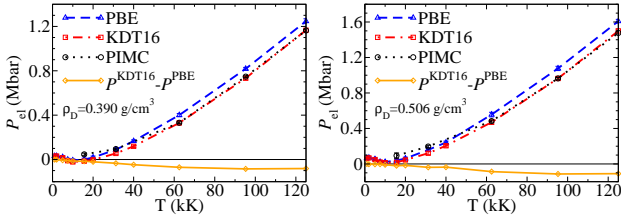


FIG. 3: Deuterium electronic pressure as a function of  $T$  for the finite-T GGA (“KDT16”) and ground-state PBE XC functionals, as well as PIMC reference results. AIMD supercell simulations,  $\Gamma$ -point only, for 128 atoms (8500 steps,  $T \leq 40 \text{ kK}$ ) or for 64 atoms (4500 steps,  $T \geq 62.5 \text{ kK}$ ).

functional for the XC free-energy. Its construction is more systematic and general than that used in the SD14 functional [13]. Thereby, the new functional provides a clear distinction between density inhomogeneity effects and  $T$ -dependence effects. A few test calculations suggest its likely utility, especially for WDM simulations. Though the new  $\mathcal{F}_{xc}^{\text{GGA}}$  has no empirical parameters, as in the case of ground-state functionals it involves design choice [24, 50, 51] regarding the gradient-expansion coefficient for  $X$  ( $\nu_x$ ) and the related parameter in  $C$  ( $\beta_c$ ).

More broadly, our analysis of the gradient expansion for finite- $T$  XC has identified appropriate explicit  $T$ -dependent variables for  $X$  and  $C$ . Together with the new parametrization of  $\tilde{B}_c(r_s, t)$ , Eq. (11), and the LDA free-energy parametrization [14], one has the constraint-based framework for GGA XC free-energy functional development. Therefore, for example, if one wished to recover a different ground-state XC functional than PBE, there is a general procedure for doing so. Virtually any ground-state GGA XC functional can be extended systematically into an XC free energy functional by use of the  $T$ -dependent variables Eq. (7) for  $X$  and Eq. (12) within the framework presented above.

*Acknowledgments.* We thank Travis Sjostrom for providing the numerical GE2 data for the XC free-energy

and for helpful comments on an earlier version of the manuscript. We thank the University of Florida Research Computing organization for computational resources and technical support. This work was supported by the U.S. Dept. of Energy BES grant de-sc0002139.

\* Electronic address: vkarasev@qtp.ufl.edu

- [1] N.D. Mermin, Phys. Rev. **137**, A1441 (1965).
- [2] M.V. Stoitsov and I.Zh. Petkov, Annals Phys. **185**, 121 (1988).
- [3] M.D. Knudson and M.P. Desjarlais, Phys. Rev. Lett. **103**, 225501 (2009).
- [4] H.R. Rüter and R. Redmer, Phys. Rev. Lett. **112**, 145007 (2014).
- [5] M.D. Knudson, M.P. Desjarlais, A. Becker, R.W. Lemke, K.R. Cochrane, M.E. Savage, D.E. Bliss, T.R. Mattsson, R. Redmer, Science, **348**, 1455 (2015).
- [6] V.V. Karasiev, D. Chakraborty, J.W. Dufty, F.E. Harris, K. Runge, and S.B. Trickey, in *Frontiers and Challenges in Warm Dense Matter*, F. Graziani et al. eds. (Springer Verlag, Heidelberg, 2014) 61.
- [7] R.N. Barnett and U. Landman, Phys. Rev. B **48**, 2081 (1993).
- [8] D. Marx and J. Hutter in *Modern Methods and Algorithms of Quantum Chemistry*, J. Grotendorst ed., John von Neumann Institute for Computing, (Jülich, NIC Series, Vol. 1, 2000) 301 and refs. therein.
- [9] J.S. Tse, Annu. Rev. Phys. Chem. **53**, 249 (2002).
- [10] *Ab Initio Molecular Dynamics: Basic Theory and Advanced Methods*, D. Marx and J. Hutter, (Cambridge University Press, Cambridge, 2009) and refs. therein.
- [11] F. Perrot and M.W.C. Dharma-wardana, Phys. Rev. A **30**, 2619 (1984).
- [12] F. Perrot and M.W.C. Dharma-wardana, Phys. Rev. B **62**, 16536 (2000); F. Perrot and M.W.C. Dharma-wardana, Phys. Rev. B **67**, 079901(E) (2003).
- [13] T. Sjostrom and J. Daligault, Phys. Rev. B **90**, 155109 (2014).
- [14] V.V. Karasiev, T. Sjostrom, J. Dufty, and S.B. Trickey, Phys. Rev. Lett. **112**, 076403 (2014).
- [15] The KSDT functional has been said to have significant XC free energy errors with respect to recent quantum Monte Carlo data for specific HEG temperatures and densities [16]. As a fraction of the total free energy, those errors are negligible however, 0.22% or less. See Supplemental Material.
- [16] T. Dornheim, S. Groth, T. Sjostrom, F.D. Malone, W.M.C. Foulkes, and M. Bonitz, Phys. Rev. Lett. **117**, 156403 (2016).
- [17] V.V. Karasiev, T. Sjostrom, and S.B. Trickey, Phys. Rev. E **86**, 056704 (2012).
- [18] V.V. Karasiev, L. Calderin, and S.B. Trickey, Phys. Rev. E **93**, 063207 (2016).
- [19] J.P. Perdew and K. Schmidt, AIP Conf. Proc. **501**, 1 (2001).
- [20] T. Sjostrom, F.E. Harris, and S.B. Trickey, Phys. Rev. B **85**, 045125 (2012).
- [21] V.V. Karasiev, T. Sjostrom, and S.B. Trickey, Phys. Rev. B **86**, 115101 (2012).
- [22] V.V. Karasiev, D. Chakraborty, O.A. Shukruto, and S.B.

- Trickey, Phys. Rev. B **88**, 161108(R) (2013).
- [23] J.C. Pacheco-Kato, J.M. del Campo, J.L. Gázquez, S.B. Trickey, and A. Vela, Chem. Phys. Lett. **651**, 268 (2016)
  - [24] J.P. Perdew, K. Burke, and M. Ernzerhof, Phys. Rev. Lett. **77**, 3865 (1996); erratum *ibid.* **78**, 1396 (1997).
  - [25] P. Hohenberg and W. Kohn, Phys. Rev. **136**, B864 (1964).
  - [26] W. Kohn and L.J. Sham, Phys. Rev. **140**, A1133 (1965).
  - [27] J.S. Blakemore, Sol. State Electr. **25**, 1067 (1982).
  - [28] J. Bartel, M. Brack, and M. Durand, Nucl. Phys. A **445**, 263 (1985).
  - [29] D.J.W. Geldart, E. Dunlap, M.L. Glasser, and M.R.A. Shegelski, Solid State Commun. **88**, 81 (1993).
  - [30] Y. Wang and J.P. Perdew, Phys. Rev. B **43**, 8911 (1991).
  - [31] F. Perrot, Phys. Rev. A **20**, 586 (1979).
  - [32] E. Dunlap, and D.J.W. Geldart, Can. J. Phys. **72**, 1 (1994).
  - [33] M.L. Glasser, D.J.W. Geldart, and E. Dunlap, Can. J. Phys. **72**, 7 (1994).
  - [34] E. Dunlap, and D.J.W. Geldart, Can. J. Phys. **72**, 14 (1994).
  - [35] D.J.W. Geldart, Top. Curr. Chem. **180**, 31 (1996).
  - [36] L. Kleinman and V. Sahni, Adv. Quantum Chem. **21**, 201 (1990) and refs. therein; E. Engel and S.H. Vosko, Phys. Rev. B **42**, 4940 (1990), erratum *ibid.* **44**, 1446 (1991).
  - [37] V.V. Karasiev, D. Chakraborty, and S.B. Trickey, Comput. Phys. Commun. **192**, 114 (2015).
  - [38] S. Pittalis, C.R. Proetto, A. Floris, A. Sanna, C. Bersier, K. Burke, and E.K.U. Gross, Phys. Rev. Lett. **107**, 163001 (2011).
  - [39] J.W. Dufty and S.B. Trickey, Mol. Phys. **114**, 988 (2016).
  - [40] E.H. Lieb, and S. Oxford, Int. J. Quantum Chem. **19**, 427 (1981).
  - [41] M. Greiner, P. Carrier, and A. Görling, Phys. Rev. B **81**, 155119 (2010).
  - [42] G. Niklasson, A. Sjölander, and K.S. Singwi, Phys. Rev. B **11**, 113 (1975).
  - [43] A.K. Gupta and K.S. Singwi, Phys. Rev. B **15**, 1801 (1977).
  - [44] E.W. Brown, B.K. Clark, J.L. DuBois, and D.M. Cepereley, Phys. Rev. Lett. **110**, 146405 (2013).
  - [45] See Supplemental Material.
  - [46] J.P. Perdew and Y. Wang, Phys. Rev. B **45**, 13244 (1992).
  - [47] J.P. Perdew, and A. Zunger, Phys. Rev. B **23**, 5048 (1981).
  - [48] Paolo Giannozzi, Stefano Baroni, Nicola Bonini, Matteo Calandra, Roberto Car, Carlo Cavazzoni, Davide Ceresoli, Guido L. Chiarotti, Matteo Cococcioni, Ismaila Dabo, Andrea Dal Corso, Stefano de Gironcoli, Stefano Fabris, Guido Fratesi, Ralph Gebauer, Uwe Gerstmann, Christos Gougoussis, Anton Kokalj, Michele Lazzeri, Layla Martin-Samos, Nicola Marzari, Francesco Mauri, Riccardo Mazzarello, Stefano Paolini, Alfredo Pasquarello, Lorenzo Paulatto, Carlo Sbraccia, Sandro Scandolo, Gabriele Scanzzero, Ari P. Seitsonen, Alexander Smogunov, Paolo Umari, and Renata M. Wentzcovitch, J. Phys.: Condens. Matter **21**, 395502 (2009).
  - [49] S.X. Hu, B. Militzer, V.N. Goncharov, and S. Skupsky, Phys. Rev. B **84** 224109 (2011).
  - [50] J.P. Perdew, A. Ruzsinszky, G.I. Csonka, O.A. Vydrov, G.E. Scuseria, L.A. Constantin, X. Zhou, and K. Burke, Phys. Rev. Lett. **100**, 136406 (2008).
  - [51] J.M. del Campo, J.L. Gázquez, S.B. Trickey, and A. Vela, J. Chem. Phys. **136**, 104108 (2012).